

ences in activation energies must be considered, and electrode polarizations must stay within a suitable range.

The model can be applied to vented batteries characterized by a small limiting current of oxygen reduction. Here, the optimum design requires high and balanced hindrance of the gassing reactions. Grid corrosion, as an aging factor, should be hindered as much as possible.

Manuscript submitted Feb. 24, 1995; revised manuscript received Nov. 22, 1995. This was Paper 155 presented at the Miami Beach, FL, Meeting of the Society, Oct. 9-14, 1994.

VARTA Batterie AG assisted in meeting the publication costs of this article.

REFERENCES

- W. Brecht, *Batter. Int.*, Issue 14, p. 80 (Jan. 1993).
- D. Berndt, E. Meissner, and W. Rusch, in *Proceedings of the 15th Intelec Meeting*, Paris, 1993, p. 139, IEEE (1993).
- U. Teutsch, in *Proceedings of the First TELESCon Meeting*, Berlin, 1994, p. 89, IEEE (1994).
- P. C. Milner, *Bell Syst. Tech. J.*, **49**, 1321 (1970).
- E. Willihnganz, *This Journal*, **126**, 1510 (1979).
- D. Berndt, *Maintenance-Free Batteries*, Research Studies Press, Taunton, Somerset, England, and John Wiley & Sons, New York (1993).
- A. J. Bard and L. R. Faulkner, *Electrochemical Methods*, p. 92, John Wiley & Sons, New York (1980).
- P. Rüetschi, R. T. Angstadt, and B. D. Cahan, *This Journal*, **106**, 547 (1959).
- M. E. Fiorino, F. J. Vaccaro, R. E. Landwehrle, in *Proceedings of the Tenth International Telecommunications Energy Conference*, San Diego, CA, p. 114 (1988).
- P. Rüetschi, *J. Power Sources*, **2**, 3 (1977/78).
- H. Rickert and J. P. Pohl, Final report of EEC Project EN3E-0144-D(8), pp. 11-13 (1989).
- E. Hämeenöja, T. Laitinen, G. Sundholm, and A. Ylipentti, *Electrochim. Acta*, **34**, 233 (1989).
- D. Pavlov, in *Power Sources for Electric Vehicles (Studies in Electrical and Electronic Engineering 11)*, B. D. McNicol and D. A. J. Rand, Editors, p. 137, Elsevier, Amsterdam (1984).
- P. Rüetschi and R. T. Angstadt, *This Journal*, **105**, 555 (1958).
- J. J. Lander, *ibid.*, **98**, 213 (1951).
- D. Marshall and W. Tiedemann, *ibid.*, **123**, 1849 (1976).
- C. E. Weinlein, J. R. Pierson, and D. Marshall, *Power Sources*, **7**, 67 (1979).
- M. Maja, P. Spinelli, *Werks. Korros.*, **36**, 554 (1985).
- A. Arlanch, G. Clerici, and M. Maja, *Power Sources*, **8**, 581 (1981).
- K. R. Bullock and W. H. Tiedemann, *This Journal*, **127**, 2112 (1980).
- E. M. L. Valeriotte, *ibid.*, **128**, 1423 (1981).
- C. S. C. Bose and N. A. Hampson, *J. Power Sources*, **189**, 261 (1987).
- J. Thompson and S. Warrell, *Power Sources*, **9**, 97 (1983).
- E. A. Khomskaya, N. F. Gorbacheva, and N. B. Tolochkov, *Sov. Electrochem.*, **16**, 48 (1980).
- C. S. C. Bose and N. A. Hampson, *Bull. Electrochem.*, **4**, 437 (1988).
- Landolt-Börnstein, *Lösungsgleichgewichte* Vol. 11, Part 2B, p. 36, Springer, Heidelberg (1962).
- W. B. Brecht, in *Proceedings of the Ninth Intelec Meeting*, Stockholm, 1987, p. 99, IEEE (1987).
- D. Berndt and E. Meissner, in *Proceedings of the Twelfth International Telecommunications Energy Conference*, Orlando, FL, p. 148 (1990).
- R. F. Nelson, *Power Sources*, **13**, 13 (1991).
- W. H. Tiedemann and J. Newman, in *Proceedings of the Symposium on Battery Design and Optimization*, S. Gross, Editor, PV 79-1, p. 23, The Electrochemical Society Proceedings Series, Princeton, NJ (1979).
- H. Gu, T. V. Nguyen, R. E. White, *This Journal*, **134**, 2953 (1987).
- D. Berndt, R. Bräutigam, and U. Teutsch, in *Proceedings of the 17th Intelec Meeting*, The Hague, 1995, p. 1, IEEE (1995).
- D. Berndt, in *Proceedings of the Seventh Intelec Meeting*, Munich, 1985, p. 125, IEEE (1985).
- W. B. Brecht, in *Proceedings of Ninth Intelec Meeting*, Stockholm, 1987, p. 99, IEEE (1987).

The Intrinsic Anodic Stability of Several Anions Comprising Solvent-Free Ionic Liquids

V. R. Koch,* L. A. Dominey,*^a and C. Nanjundiah*

Covalent Associates, Incorporated, Woburn, Massachusetts 01801, USA

M. J. Ondrechen^b

Department of Chemistry, Northeastern University, Boston, Massachusetts 02115, USA
and

Department of Chemistry, Aarhus University, DK-8000 Aarhus C, Denmark

ABSTRACT

Salts of the form 1,2-dimethyl-3-propylimidazolium X [where X = AsF₆⁻, PF₆⁻, (CF₃SO₂)₂N⁻, and (CF₃SO₂)₃C⁻] were prepared and purified. Linear sweep voltammetry was conducted at 80°C, a temperature at which all four salts were molten, at Pt, W, and glassy carbon working electrodes. We found that the intrinsic anodic stability of these anions was in the order (CF₃SO₂)₃C⁻ > (CF₃SO₂)₂N⁻ ~ AsF₆⁻ > PF₆⁻. These experimental solution-phase oxidation potentials correlated well with gas-phase highest occupied molecular orbital energies calculated by an *ab initio* technique.

The advent of lithium-ion or "rocking chair" rechargeable battery technology has severely stretched the anodic limits of common nonaqueous electrolytes. Thus, the onset of electrolyte oxidation often defines the cutoff voltage on

charge prior to accessing the full capacity of the cathode. In this regard, transition metal oxide cathodes of the form LiMO₂ (M = Co, Ni, and Mn) may be delithiated to the point where cell potentials readily exceed 4 V vs. Li⁺/Li, especially at the high rates.¹ This in turn exposes both the organic solvent(s) and the anion of the supporting electrolyte to cathode voltages in excess of 4 V. Indeed, a cathode potential of 4.3 V is energetically equivalent to 418.6 kJ/mol which is sufficiently energetic to break C-H

* Electrochemical Society Active Member.

^a Present address: OM Group, Inc., Cleveland, OH 44113, USA.

^b Present address: Northeastern University, Boston, MA 02115, USA.

and C-O bonds² which comprise both cyclic and acyclic carbonate solvents favored in lithium-ion battery technology.¹ The anodic polymerization of propylene carbonate at a LiCoO₂ electrode on charge was first reported by Goodenough and co-workers.³ Since then, manufacturers of lithium-ion batteries have restricted single-cell excursions beyond the electrolyte's oxidation potential by attaching ancillary electronics.⁴

The proclivity of an electrolyte to undergo irreversible oxidation chemistry on charge is exacerbated by the need to store fully charged batteries at elevated temperatures of up to 70°C for long periods of time. Since a 10°C increase in temperature roughly doubles the rate of a pseudo-first order (heterogeneous) reaction, 70°C storage increases cathode/electrolyte redox kinetics by a factor of 32 over that experienced at room temperature.

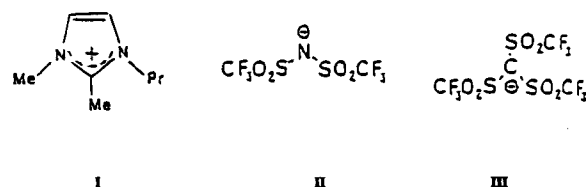
Guyomard and Tarascon have addressed the problem of oxidative electrolyte stability at elevated temperatures in lithium-ion cells containing a LiMn₂O₄ cathode.⁵ Their electrolyte of choice, a 1 mol · dm⁻³ LiPF₆/ethylene carbonate:dimethyl carbonate (50:50 v/o), was found to be oxidatively stable to 4.9 V at room temperature and to 4.8 V at 55°C.⁶

However, when spirally wound Li_xC/LiMn₂O₄ AA cells charged to 4.3 V were stored at 70°C, significant electrolyte oxidation was detected after only 3 days.^{5b} Whether the source of the observed oxidation current was one or both solvents and/or PF₆⁻ was not addressed. Later work by Guyomard and Tarascon considered the problem of the room temperature breakdown voltage of electrolytes comprising either 1 mol · dm⁻³ LiX/ethylene carbonate:diethoxyethane (50:50 v/o) or 1 mol · dm⁻³ LiX/ethylene carbonate:dimethyl carbonate (50:50 v/o) as a function of anion.⁶ For this study X = ClO₄⁻, PF₆⁻, BF₄⁻, AsF₆⁻, (CF₃SO₂)₂N⁻, and CF₃SO₃⁻, and the electrode was a LiMn₂O₄ composite incorporating a binder and carbon black. A two-electrode galvanostatic test procedure was employed for this study. The former solvent system gave an anion stability order of ClO₄⁻ > (CF₃SO₂)₂N⁻ > CF₃SO₃⁻ > AsF₆⁻ > PF₆⁻ > BF₄⁻; the latter solvent system gave ClO₄⁻ ≅ PF₆⁻ ≅ BF₄⁻ > AsF₆⁻ > (CF₃SO₂)₂N⁻ > CF₃SO₃⁻. Clearly the choice of either diethoxyethane or dimethyl carbonate as a cosolvent dramatically influences both electrolyte and anion stabilities in an unpredictable manner.

Our concern with anion stability has led to the development of the tris(trifluoromethylsulfonyl) methide anion patented by Dominey⁷ and discussed in a review article on nonaqueous electrolytes.⁸ In liquid electrolytes, the methide anion has proven to be electrochemically robust to beyond 4 V vs. Li⁺/Li, but the species eventually undergoing oxidation was not determined.⁹ Cyclic voltammetry experiments conducted on Pt by Ciemiecki and Auburn showed that in 0.1 mol · dm⁻³ LiX/CH₃CN (where X = AsF₆⁻, PF₆⁻, BF₄⁻, and CF₃SO₃⁻) the onset of oxidation occurred at more or less the same potential which precluded any insights into anion stability.¹⁰ Ue and co-workers determined the limiting oxidation and reduction potentials of electrolytes composed of quaternary ammonium anion salts and common organic solvents.¹¹ They found that BF₄⁻ and PF₆⁻ were more resistant to oxidation compared to ClO₄⁻ and CF₃SO₃⁻ in propylene carbonate, but no other distinctions were made.

To unambiguously resolve the problem of initial solvent oxidation or concurrent solvent and anion oxidation, we set out to investigate the intrinsic oxidative stability of four anions of interest to the Li battery community by way of electrochemical studies in the absence of solvent. This was accomplished by preparing a set of highly purified salts consisting of a common organic cation, i.e., 1,2-dimethyl-3-propylimidazolium (DMPI) (I), and the following anions: AsF₆⁻, PF₆⁻, bis(trifluoromethylsulfonyl) imide (Im⁻) (II), and tris(trifluoromethylsulfonyl) methide (Me⁻) (III). While DMPIIm and DMPIMe were fluid at room temperature, DMPIAsF₆ and DMPIPF₆ were not. Accordingly, our electrochemical investigation of these salts was conducted at 80°C, some 8°C beyond the melting point

of DMPIPF₆, and 22°C beyond the melting point of DMPIAsF₆.



Scheme 1.

The experimentally determined intrinsic oxidation potentials of AsF₆⁻, PF₆⁻, Im⁻, and Me⁻ were correlated with the energy of the highest occupied molecular orbital (HOMO) calculated for each anion by way of an *ab initio* density functional theory (DFT) method.¹² In this method, the molecular orbitals comprising each anion are expressed in the usual linear combination of atomic orbitals (LCAO) fashion and the Schrödinger equation is solved self-consistently. The ionization potentials (IP) for each anion were calculated by a transition operator (TO) technique. Atomic coordinates were taken from single-crystal x-ray structural determinations rather than from molecular geometry optimization techniques. These coordinates were subsequently used in our *ab initio* calculations.

Experimental

General.—All electrochemical experiments were conducted in a Vacuum Atmospheres Company glove box under an Ar atmosphere. The glove box atmosphere was continuously recirculated through a Model HE-493 Dri-train which scavenged H₂O and O₂. The H₂O and O₂ content of the glove box was typically less than 10 ppm. IR spectra were collected on an IBM FT/32 optical bench (MCT detector) running under an IBM-compatible PC equipped with Nicolet software.

Preparation of DMPIX.—The four new salts were prepared by a metathesis reaction in acetonitrile (AN) (Fisher, HPLC grade) in accordance with Eq. 1



DMPICl was prepared and purified according to the method of Gifford and Palmisano.¹³ LiAsF₆ (Lithco, battery grade), LiPF₆ (Hashimoto), and LiIm (3M Company) were used without further purification. LiMe (mp 272 to 273°C) was prepared by the neutralization of the parent acid [tris(trifluoromethylsulfonyl)methane, 3M Company] with Cs₂CO₃ followed by metathesis of the CsMe salt to LiMe via LiCl in anhydrous THF (Fisher, HPLC grade). LiMe was purified by dissolution in hot deionized H₂O followed by refluxing with activated charcoal. After filtration with Celite filter aid, the H₂O was removed *in vacuo* leaving pure LiMe.

All DMPIX reaction mixtures in AN were cold-vacuum filtered to remove LiCl. The AN was removed *in vacuo* and the DMPIX residue taken up in CH₂Cl₂. This solution was extracted with deionized H₂O to remove residual LiCl. When the aqueous phase tested negative for Cl⁻ via an aqueous AgNO₃ solution, the organic phase was dried over MgSO₄, filtered, and the CH₂Cl₂ removed under reduced pressure. The residual salt was dried *in vacuo* at 80°C for 16 h. If at this point the salt was not white (X = AsF₆⁻ or PF₆⁻) or a colorless oil (X = Im⁻ or Me⁻), DMPIX was taken up in dry CH₂Cl₂ and refluxed with activated charcoal for 4 h. After the addition of Celite the mixture was vacuum filtered through a Whatman GF/F 0.7 µm filter disk and the solution was treated as before. All DMPIX yields exceeded 90%. Fourier transform infrared (FTIR) spectra of DMPIX were essentially identical to an overlay of the FTIR spectra of DMPICl and LiX. The melting points for DMPIAsF₆ and DMPIPF₆ were 57 to 58°C and 71 to 72°C, respectively. The water content of a known amount of DMPIX dissolved in anhydrous MeOH was measured by a Mettler Model DL 18 Karl Fischer Titrator and found to range from 25 to 40 ppm.

Electrochemical cells and instrumentation.—Both linear sweep and cyclic voltammetry (CV) were accomplished in a Brinkmann three-electrode cell (Model EA 875-1/6). For work conducted at elevated temperature, this cell was thermostated to $80 \pm 1^\circ\text{C}$ by way of a heating mantle, a Type J thermocouple inserted into a Pyrex sleeve which was dipped into the molten salt, and an Omega 400/JC temperature controller. The working electrodes were polished disks ($0.1 \mu\text{m}$ alumina) of glassy carbon (0.07 cm^2), and Pt (0.21 cm^2) sealed in Pyrex, or W (0.07 cm^2) sealed in uranium glass. Both the reference and counterelectrodes were pieces of 10 mil Li foil (Foote). The stability of Li metal to DMPIX ($\text{X} = \text{Im}^-$ and Me^-) was the subject of a previous publication.¹⁴ In order to insure a stable, reproducible Li^+/Li reference potential, enough LiAsF_6 , LiPF_6 , LiIm , and LiMe were added to their respective DMPIX ionic liquid to form a $20 \times 10^{-3} \text{ mol} \cdot \text{dm}^{-3}$ solution. Both cyclic and linear sweep voltammetry were accomplished via an EG&G Princeton Applied Research 273 potentiostat/galvanostat interfaced with an IBM compatible personal computer running under EG&G M270 software.

The “anodic stability” was arbitrarily defined as the potential at which the current density reached $1 \text{ mA}/\text{cm}^2$ at a sweep rate of $20 \text{ mV}/\text{s}$. Electrolyte resistance between reference and working electrode was obtained from the current response of a 25 mV pulse. Corrections for iR drop were automatically accomplished by a positive feedback technique in accordance with protocols built into the EG&G M270 software. Corrections less than 10 mV corrections were neglected. All potentials are referenced with respect to the Li^+/Li couple unless otherwise noted.

Results and Discussion

Electrochemistry of solvent-free ionic liquids.—Figure 1 shows a CV of DMPIIme at 22°C conducted at a glassy carbon working electrode. On scanning in the negative direction from the rest potential, we found that the DMPI^+ cation began to reduce irreversibly at $0.63 \text{ V vs. Li}^+/\text{Li}$. A previously reported reduction potential for DMPI^+ on glassy carbon in a $\text{DMPICl}:\text{AlCl}_3$ (1:1 m/o) room temperature molten salt was $-2.45 \text{ vs. Al}^{+3}/\text{Al}$.¹² When adjusted to the Li potential,¹⁰ this value becomes 0.69 V in good agreement with our observation. On going in the positive direction, we observed the onset of irreversible oxidation at 5.21 V , presumably due to the methide anion. Within the electrochemical window shown in Fig. 1, the glassy carbon working electrode started to passivate after four to five cycles. The electrode activity was easily restored by scrubbing the glassy carbon disk with a Kimwipe® paper tissue.

We next investigated the anodic behavior of the four DMPIX salts at 80°C . In addition to glassy carbon, we also employed Pt and W disk working electrodes. At least three linear sweep voltammograms were collected at each electrode for each salt at 80°C . The reproducibility was $\pm 20 \text{ mV}$ for a given electrode in a given salt. Figure 2

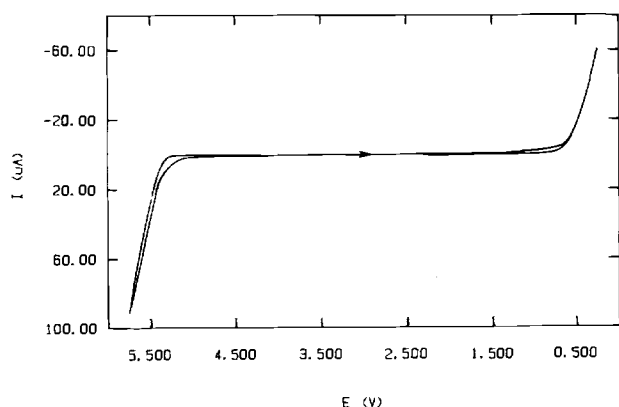


Fig. 1. CV of DMPIIme on glassy carbon at 22°C ; $\nu = 20 \text{ mV}/\text{s}$, $A = 0.07 \text{ cm}^2$.

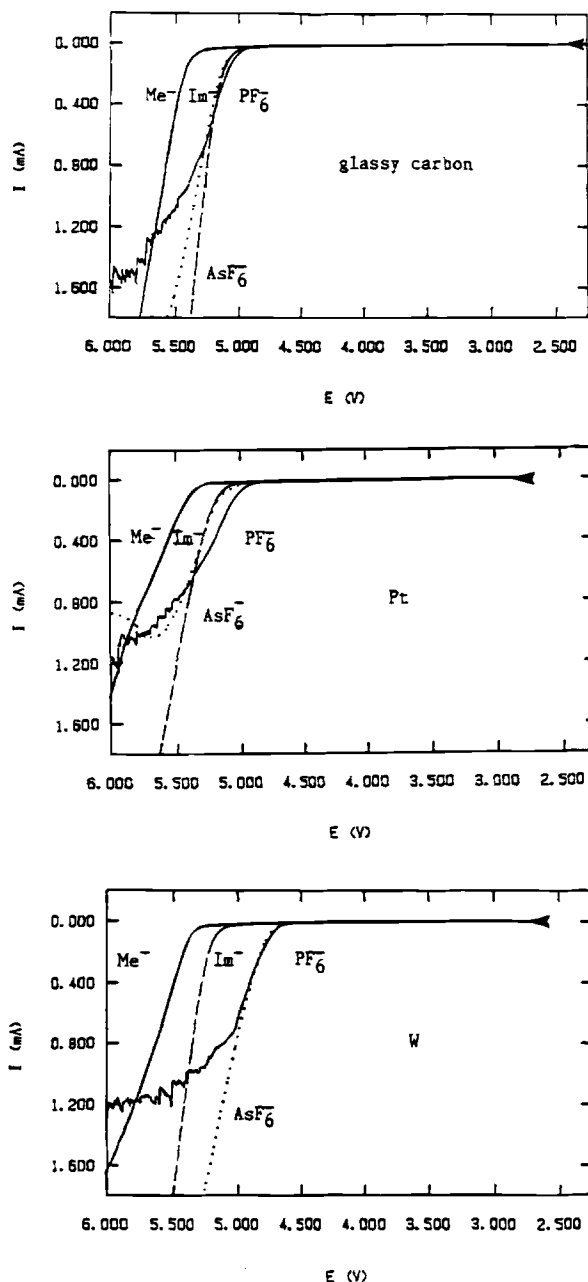


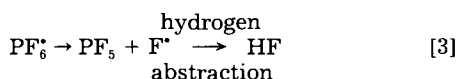
Fig. 2. Linear sweep voltammograms of DMPIX at 80°C (where $\text{X} = \text{AsF}_6^-$, PF_6^- , Im^- , and Me^-) on (a) glassy carbon, (b) Pt, and (c) W; $\nu = 20 \text{ mV}/\text{s}$.

shows an overlay of linear sweep voltammograms for each of the four salts at three different electrodes. The oxidation currents obtained at Pt were normalized to 0.07 cm^2 , the area of the glassy carbon and W electrodes.

At all three electrodes DMPIIme manifested the highest anodic stability followed by DMPIIm. The PF_6^- - and AsF_6^- -based ionic liquids have similar stabilities on W (*vide infra*), while the DMPIAsF_6 was more stable than DMPIPF_6 on Pt and glassy carbon. Also of interest was the noise seen in the DMPIPF_6 voltammograms positive of about 5.5 V on all three electrodes. By potentiostating each working electrode at 5.75 V in DMPIPF_6 we observed a gas bubble form and grow on the electrode surface. The gas was collected in an IR gas cell equipped with KBr windows and subjected to FTIR analysis from 4000 to 600 cm^{-1} , the limit of our MCT detector. We found three absorption bands at 1031 , 994 , and 864 cm^{-1} .

It is well known that unsolvated LiPF_6 is susceptible to decomposition into LiF and PF_5 at elevated tempera-

tures,¹⁵ but this decomposition is not caused by the oxidation of PF₆⁻. Along these lines, Carlin and co-workers reported on the intercalation of PF₆⁻ into graphite at 90°C from a 1-methyl-3-ethylimidazolium⁺ (MEI⁺) PF₆⁻ solvent-free ionic liquid at a potential of 1.3 V *vs.* Al³⁺/Al,¹⁶ which corresponds to 4.44 V *vs.* Li⁺/Li. No gassing of the melt at the graphite electrode was reported in accordance with our observations from linear sweep voltammetry in the potential regime between 5.5 and 2.75 V. In order to explain the gas evolution, we suggest that the PF₆⁻ anion is electrochemically oxidized to the PF₆[•] radical with subsequent decomposition to gaseous PF₅ and HF as shown in Eq. 2 and 3



PF₅ manifests two strong fundamental bands in the infrared at 947 and 575 cm⁻¹,¹⁷ the first of which was not observed in our FTIR spectrum, while the latter was not accessible to our instrument. Similarly, the strong 4138 cm⁻¹ band for HF was also not observed in the FTIR spectrum of our gas sample. However, both PF₅ and HF are known to be highly reactive with glass forming SiF₄ [lit. 1031 and 390 cm⁻¹ ^{17,18}]. Additionally, PF₅ can react with adventitious water to form POH₃ (lit. 990 and 873 cm⁻¹) as well as HF.¹⁹ We believe that our FTIR spectra of the gas sample was comprised of SiF₄ and POH₃ by-products resulting from the reactivity of PF₅ and HF with our FTIR gas cell in accordance with what has been observed previously.¹⁸

The oxidation potentials for these salts are presented in Table I. On both glassy carbon and Pt the spread between DMPiPF₆ and DMPiMe oxidation is 350 to 400 mV or about 33.5 kJ/mol. A smaller difference (~100 mV) exists between DMPiAsF₆ and DMPiPF₆ on both glassy carbon and Pt. Interestingly, both DMPiPF₆ and DMPiAsF₆ manifest unusually low oxidation potentials on W.

We must now consider whether the source of the observed anodic current is, indeed, the anion of the ionic liquid. Assuming for a moment that DMPI⁺ oxidizes negative of the four anions, what kind of current-voltage response would be expected? Since DMPI⁺ is common to the four salts one would expect to see no difference in the current-voltage response from one salt to the next. A linear sweep voltammogram at a potential negative of 4.8 V and identical to all four salts would result. But because we see four distinct voltammograms, the oxidation of DMPI⁺ cannot be the source of the anodic current for X = PF₆⁻, AsF₆⁻, and Im⁻. However, with the data at hand we cannot unambiguously distinguish between DMPI⁺ and Me⁻ as the source of the anodic current in DMPiMe.

To address this question, a linear sweep voltammogram at glassy carbon in molten CsMe (mp 232 to 233°C) was obtained at 240°C. The onset of anodic current, the source of which must be Me⁻ since Cs⁺ is in its highest oxidation state, was compared to that obtained at glassy carbon in DMPiMe also heated to 240°C. Because this temperature exceeds the melting point of Li by some 80°C, a quasi-Pt reference electrode was used in both cases. Within experimental error (±10 mV), we found that the two voltammograms superimposed indicating that Me⁻ does not oxidize

Table II. Effect of temperature on the oxidation limits (E_o) and the reduction limits (E_r) of DMPIX.^a

X	T (±1°C)	E _o (±0.02 V)	E _r (±0.02 V)	Electrochemical window, ΔV (±0.04 V)
Im ⁻	22	5.40	0.20	5.20
Me ⁻	22	5.65	0.28	5.37
Im ⁻	80	5.06	0.51	4.55
Me ⁻	80	5.34	0.44	4.90
Me ⁻	240	4.97 ^b	~2.0 ^b	~2.97

^a When *i*_a = 1 mA/cm² on glassy carbon; *v* = 20 mV/s.

^b Measured with respect to a quasi-Pt reference and corrected to a Li⁺/Li scale.

positive of DMPI⁺. Taken together, these data, free of the influence of solvent, accurately reflect the relative order of intrinsic oxidative stabilities of AsF₆⁻, PF₆⁻, Im⁻, and Me⁻ in the liquid state with DMPI⁺ as the counterion.

The effect of temperature on the electrochemical window of DMPIX.—Because DMPiIm and DMPiMe are fluid at room temperature, and because we obtained electrochemical data on DMPiMe at 240°C, we decided to examine the effect of temperature on the width of the electrochemical window. Table II collects the data available for Im⁻ and Me⁻ at 22 and 80°C, and for Me⁻ at 240°C. On going from 22 to 80°C the available electrochemical window contracts by about 30 mV at each end for both Im⁻ and Me⁻ in accordance with the formalism of the Nernst equation. The magnitude of window contraction for these observations is quite different from that reported previously for linear sweep voltammograms conducted at glassy carbon in 0.65 mol · dm⁻³ Et₄NBF₄/propylene carbonate.¹¹ When the temperature was increased from 25 to 75°C in the solvent plus salt electrolyte, the electrochemical window contracted by about 650 mV at a current density of 1 mA/cm²,¹¹ the same current density used in our experiment. This suggests that solvent-free ionic liquids may better maintain the limits of their electrochemical windows at elevated temperatures compared to traditional electrolytes. When the temperature of DMPiMe was raised from 80 to 240°C the anodic end of the window lost about 340 mV compared to the 80°C value while the cathodic limit shifted about 1500 mV in the positive direction. We believe that this anomalously large potential shift may be ascribed to the formation of DMPI⁺ decomposition products rather than the reduction of DMPI⁺ itself as the DMPiMe, clear and colorless at 80°C, slowly turned dark yellow at 240°C. In support of this speculation is the fact that decomposition of the analogous MEI⁺ cation in MEIAlCl₄ occurs at about 270°C,¹⁹ while the Me⁻ anion itself is known to decompose at 340°C in molten LiMe.⁹

Ab initio calculations on the electronic structures of AsF₆⁻, PF₆⁻, Im⁻, and Me⁻.—It is of interest to attempt to correlate the electrochemical oxidation potentials of these anions with their respective HOMO energies as has been done previously with neutral organic molecules.^{20,21} More recently, Kita has correlated the electrochemical oxidation potential of a series of five tetra-aryl lithium borate salts in propylene carbonate with their HOMO energies calculated by a modified neglect of differential overlap (MNDO) approach.²² The oxidation potentials were determined by Horowitz and co-workers at Exxon.²³ An excellent fit was obtained. Rather than using the semi-empirical MNDO approach, we employed *ab initio* density functional theory which is similar to a Hartree-Fock calculation, except that the exchange operator is replaced by an exchange and correlation potential, *V*_{xc}.¹² This potential depends upon a local electron density functional. In this method the molecular orbitals comprising each anion are expressed in the usual LCAO fashion and the Schrödinger equation is solved self-consistently. A numerical basis set is optimized

Table I. Oxidation potentials of DMPIX salts at 1 mA/cm².

X	E _o , Working electrode ±0.02 V ^a		
	Glassy Carbon	W	Pt
PF ₆ ⁻	4.94	4.72	5.00
AsF ₆ ⁻	5.05	4.75	5.10
Im ⁻	5.06	5.16	5.13
Me ⁻	5.34	5.34	5.35

^a *vs.* Li⁺/Li at 80°C.

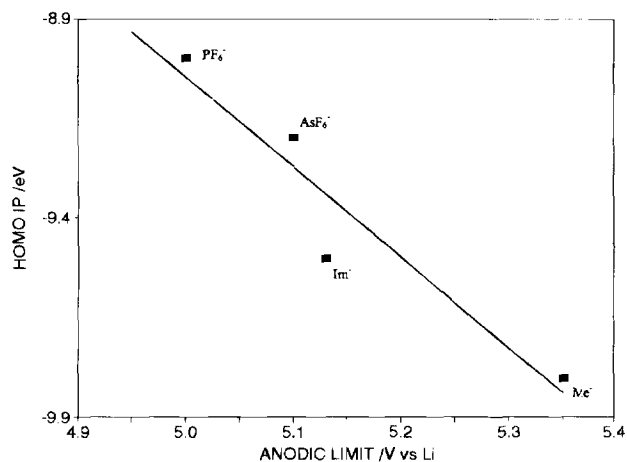


Fig. 3. Plot of calculated HOMO ionization potential energies against experimental oxidation potentials determined at Pt for DMPIX ($X = \text{AsF}_6^-$, PF_6^- , Im^- , and Me^-). The correlation coefficient is 0.91.

for each anion of interest and consists of the set of atomic orbitals appropriate for each anion.

The basis set includes the 1s-2s and 2p functions on all C, O, and F atoms; the 1s-3s and 2p-3p functions on the N atom of imide; the 1s-3s, 2p-3p, and 3d functions on the S and P atoms; and 1s-4s, 2p-4p, and 3d-4d on the As atom. Each set of functions is optimized separately for each anion.

We wish to compare the HOMO energies with the experimental oxidation potentials. However, Koopmans' theorem^{24,25} is not valid in the DFT scheme. (Koopmans' theorem states that the negative of the Hartree-Fock energy eigenvalue for each orbital in the molecular ground state is equal to the ionization potential of that orbital.) Therefore we calculated the IP for the HOMO of each anion using a TO method.²⁵ Hence, the negative of our calculated ionization potential is equivalent to the orbital energy in the Hartree-Fock scheme. The reported HOMO energies are thus calculated as-IP; these are expected to be more reliable than the calculated ground-state energy eigenvalues. Atomic coordinates were obtained from x-ray crystallographic data.²⁷⁻³⁰

Figure 3 presents a plot of the experimentally obtained oxidation potentials on Pt against the calculated HOMO energies obtained from the TO technique. The correlation is reasonable with a calculated correlation coefficient of 0.91. Table III compares previously published HOMO energies for the triflate [Tf^- , (CF_3SO_3^-)] anion as well as Im^- and Me^- . Kita *et al.* used a semi-empirical MNDO method²² and Sanchez *et al.* assumed interatomic bond lengths in their work.³⁰ Our approach used an *ab initio* method together with crystallographic data for the bond lengths of the particular anions of interest, and, therefore, we believe our data to be the most accurate. Nonetheless, the trend for Tf^- , Im^- , and Me^- is consistent across the three groups of data. To our knowledge, Me^- has both the lowest lying

Table III. Calculated HOMO energies for several anions.

Anion	Calculated HOMO energies in eV		
	Kita <i>et al.</i> ^a	Sanchez <i>et al.</i> ^b	This paper ^c
PF_6^-	—	—	-9.0
AsF_6^-	—	—	-9.2
Tf^-	-6.96	-7.48	—
Im^-	-8.19	-8.52	-9.5
Me^-	-8.70	—	-9.8

^a Ref. 22.

^b Ref. 30.

^c HOMO ionization potential.

HOMO energy calculated and the highest experimentally determined oxidational potential of any organic anion.

Conclusions

This work has shown how the intrinsic anodic stability of four different anionic species may be unambiguously determined in DMPI⁺-based solvent-free ionic liquids. The CF_3SO_3^- -derived organic anions, Im^- and Me^- were found to have higher oxidation potentials than either AsF_6^- or PF_6^- . A modest loss in the electrochemical window of DMPIIm and DMPIMe was found when the temperature was increased from 22 to 80°C. The Me^- anion, with the highest oxidative stability measured to date, is particularly attractive for use as a supporting electrolyte in electrochemical devices where high anodic limits and thermochemical stability are particularly important. Finally, we were able to correlate the experimental oxidation potentials with their respective HOMO energies calculated by an *ab initio* DFT-TO technique.

Acknowledgments

This work was funded in part by the Army Research Office under DoD Contract No. DAAL03-92-C-0038. M. J. O. acknowledges the hospitality of Professor Jan Linderberg of Aarhus University (Aarhus, Denmark) where part of this work was accomplished. We thank Professor D. Desmarteau for the crystallographic data on the imiole species prior to publication.

Manuscript submitted June 5, 1995; revised manuscript received Oct. 9, 1995.

REFERENCES

- S. Megahed and B. Scrosati, *J. Power Sources*, **51**, 79 (1994), and references therein.
- J. March, *Advanced Organic Chemistry*, 3rd ed., pp. 21-23, Wiley-Interscience, New York (1985).
- M. Mizushima, P. C. Jones, P. J. Wiseman, and J. B. Goodenough, *Solid State Ionics*, **314**, 171 (1981).
- K. Ozawa and T. Aita, in Extended Abstract of the 11th International Seminar on Primary and Secondary Battery Technology Applications, Deerfield Beach, FL, Feb. 28- Mar. 3, 1994.
- (a) D. Guyomard and J. M. Tarascon, *This Journal*, **139**, 937 (1992); (b) *ibid.*, **140**, 3071 (1993).
- D. Guyomard and J. M. Tarascon, *J. Power Sources*, **54**, 92 (1995).
- L. A. Dominey, U.S. Pat. 5,273,840 (1993).
- L. A. Dominey, in *Lithium Batteries: New Materials, Developments and Perspectives*, G. Pistoia, Editor, pp. 149-152, Elsevier, Amsterdam (1994).
- L. A. Dominey, V. R. Koch, and T. J. Blakley, *Electrochim. Acta*, **37**, 1551 (1992).
- K. T. Ciemiecki and J. J. Auburn, in *Lithium Batteries*, A. N. Dey, Editor, PV 84-1, p. 363-373, The Electrochemical Society Proceedings Series, Pennington, NJ (1984).
- M. Ue, K. Ida, and S. Mori, *This Journal*, **141**, 2989 (1994).
- J. K. Labanowski and J. W. Andzelm, *Density Functional Methods in Chemistry*, Springer-Verlag, New York (1994), and references therein.
- P. R. Gifford and J. B. Palmisano, *This Journal*, **134**, 610 (1987).
- V. R. Koch, C. Nanjundiah, G. B. Appetecchi, and B. Scrosati, *ibid.*, **142**, L116 (1995).
- R. A. Wiesbock, U.S. Pat. 3,654,330 (1972).
- R. T. Carlin, H. D. De Long, J. Fuller, and P. C. Truelove, *This Journal*, **141**, C73 (1994).
- L. C. Hoskins, *J. Chem. Phys.*, **42**, 2631 (1965).
- L. C. Hoskins and R. C. Lord, *ibid.*, **46**, 2402 (1967).
- J. R. Stoff, *Thermochim. Acta*, **152**, 421 (1989).
- M. J. S. Dewar, J. A. Hashmall, and N. Trinajstić, *J. Am. Chem. Soc.*, **93**, 5555 (1970), and references therein.
- L. L. Miller, G. D. Nordblom, and E. D. Mayeda, *J. Org. Chem.*, **37**, 916 (1972).
- F. Kita, A. Kawakami, T. Sonoda, and H. Kobayashi, in *New Sealed Rechargeable Batteries and Supercapacitors*, B. M. Barnett, E. Dowgiallo, G. Halpert,

- Y. Matsuda, and Z-i. Takehara, Editors, PV 93-23, p. 321, The Electrochemical Society Proceedings Series, Pennington, NJ (1993).
23. H. H. Horowitz, J. I. Haberman, L. P. Klemann, G. H. Newman, E. L. Stogryn, and T. A. Whitney, in *Lithium Batteries*, H. V. Venkatesetty, Editor, PV 81-4, p. 131-143, The Electrochemical Society Proceedings Series, Pennington, NJ (1981).
24. T. A. Koopmans, *Physica*, **1**, 104 (1933).
25. J. C. Slater, *Adv. Quantum Chem.*, **6**, 1 (1972).
26. J. Fuller, R. T. Carlin, H. C. De Long, and D. Haworth, *J. Chem. Soc., Chem. Commun.*, 299 (1994).
27. (a) R. J. Gillespie *et al.*, *Inorg. Chem.*, **10**, 2781 (1971); (b) R. J. Gillespie, H. Lynton, and J. Passmore, *Can. J. Chem.*, **49**, 2539 (1971).
28. D. D. Desmarteau, Personal communication.
29. L. Turowsky and K. Seppelt, *Inorg. Chem.*, **27**, 2135 (1988).
30. D. Benrabah, R. Arnaud, and J-Y. Sanchez, Paper presented at the Fourth International Symposium on

Predictions from the Macrohomogeneous Model of an Aerospace Ni-Cd Battery

B. V. Ratnakumar,* P. Timmerman,* C. Sanchez, S. Di Stefano,* and G. Halpert*

Jet Propulsion Laboratory, California Institute of Technology, Pasadena, California 91109, USA

ABSTRACT

The mathematical porous-electrode model developed at Texas A&M University has been combined with a planar model for the surface active layer to formulate a pseudo two-dimensional model for a sealed nickel-cadmium cell. The porous electrode model is based on a macrohomogeneous description of the electrodes and takes into account various processes such as mass transport in the liquid phase and porosity and conductivity changes in the solid phase. The planar electrode model describes the processes occurring across the surface layer of active material, *i.e.*, solid-state diffusion of protons and conductivity changes in the nickel oxide, and the charge-transfer across the film-electrolyte interface. Also, various routines have been added to the pseudo two-dimensional model thus integrated, to allow predictions for any nickel-cadmium battery under any desired charge-discharge schedule. From a comparison with the experimental data of an aerospace cell, the model parameters describing charge-discharge behavior of a Ni-Cd cell have been optimized to obtain a closer prediction with the experimental data. Upon optimizing the model parameters, the performance of the aerospace nickel-cadmium cell has been simulated under various experimental conditions, *i.e.*, at different rates and temperatures. Also, generic Ragone plots for the cell and typical Tafel plots for cadmium and nickel electrodes at different states of charge have been constructed from the simulations. Finally, this model has been made available for any interested user through COSMIC NASA's Computer Management and Information Center, along with documentation in six volumes describing the code, principles, and operating instructions.

Introduction

Prediction of battery performance through simulated tests using appropriate models would provide useful guidelines for a proper management of a power subsystem on a spacecraft. JPL has been involved for the past few years in the development of mathematical models for aerospace sealed nickel-cadmium and nickel-hydrogen rechargeable cells. These battery models have been built around the cell models developed at Texas A&M University and University of South Carolina. The cell models utilize the macrohomogeneous approach of Newman,¹ *i.e.*, volume averaging distributed quantities such as porosity and conductivity over homogeneous mixtures of electrode and electrolyte phases. Various aspects addressed in the cell model include: (i) material balance for the dissolved species generated/consumed by the electrochemical reaction and transported by diffusion and migration, (ii) variations in the electrode porosity due to differences in the molar volume of the reactants and products, (iii) changes in the electrochemical potential in the solid phase or in the electrolyte, (iv) charge-transfer kinetics through a generalized Butler-Volmer rate equation, (v) principles of conservation of charge in the electrochemical cell, and (vi) effects of intercalation and slow diffusion of protons into the positive electrode. The governing equations for the above phenomena are solved for each of the regions (positive electrode, separator, and negative electrode) with appropriate boundary and initial conditions by a finite-difference approach using the Pentadiagonal or Tridiagonal BAND-J method.² Similar mathematical models based on the above macrohomogeneous approach, have been developed by White *et al.*, for various electrochemi-

cal systems such as lead-acid,^{3,4} nickel-cadmium,⁵⁻⁷ nickel-hydrogen,^{8,9} lithium rechargeable cells containing intercalation cathodes,¹⁰ and hydrogen-oxygen fuel cell.¹¹

Specifically for the nickel-cadmium rechargeable cell, the macrohomogeneous approach has been adopted by various investigators to map the distribution of the reaction currents, electrode potentials, and species concentrations in one direction (hence called one-dimensional models), *i.e.*, perpendicular to the current collectors.^{5-7,12} The omission of the polarization effects caused by the nickel oxyhydroxide/hydroxide film in these earlier versions yielded smaller overpotentials, flatter discharge curves, and higher utilizations for the Ni oxide electrode than are actually observed. Subsequently, two-dimensional macrohomogeneous models have been developed by accounting for the changes in the proton concentration and electronic conductivity across the active nickel hydroxide film, during charge and discharge.^{9,13} These two-dimensional models require rather sophisticated computing facilities and used to be run on supercomputers and mainframe computers, but now can be implemented on workstations.

Concurrently, a simplified approach has been proposed by JPL in collaboration with Weidner of the University of South Carolina,¹⁴ which involves an analytical solution for the proton diffusion and variable electronic conductivity across the positive active material layer. The planar treatment of the Ni electrode is justified by the minimal concentration changes occurring in the solution during charge/discharge as compared to the solid phase. The Ni-Cd cell model based on the simplified planar treatment for the Ni electrode can be implemented on a personal computer. This simplified solid-phase treatment has subsequently been used in conjunction with the one-dimensional macrohomogeneous porous-electrode model of Texas A&M University to develop the present pseudo two-di-

* Electrochemical Society Active Member.